

# Onset of Synchronization in Complex Networks of Noisy Oscillators

Bernard Sonnenschein\* and Lutz Schimansky-Geier

*Department of Physics, Humboldt-Universität zu Berlin,  
Newtonstr. 15, 12489 Berlin, Germany; and*

*Bernstein Center for Computational Neuroscience Berlin, Philippstr. 13, 10115 Berlin, Germany*

We investigate the synchronization of phase oscillators with diverse frequencies on random networks. Each of the oscillators is driven by Gaussian white noise and the diversity of the oscillators is due to a corresponding frequency distribution. The structure of the network is quantified by the given degree distribution of the nodes. We approximate the network by a cluster of nodes that are all-to-all coupled and whose edges are weighted. Within this model we are able to formulate the effective dynamics for a single oscillator and to derive the corresponding Fokker-Planck equation. The latter allows in a self-consistent way to calculate the critical coupling strength for the onset of synchronized oscillation in the network. It is given as a product of two factors, where the first one depends solely on the network topology, while the second factor is a function of the noise intensity and the diversity of the oscillators. Our result is applied to a dense small-world network model and corroborated by numerical simulations.

PACS numbers: 05.40.-a, 05.45.Xt, 87.10.Ca, 87.19.lj

## I. INTRODUCTION

Synchronization phenomena have been observed in many different fields such as the chaotic intensity fluctuations of coupled lasers [1], flashing swarms of fireflies [2], spiking dynamics of neurons [3–6], pacemaker cells in the heart [7], and the menstrual cycles of women living together [8–10], to mention only a few examples. Without doubts, the phenomenon of synchronization is a central mechanism in physics, chemistry, biology, and medicine as reported impressively in various monographs [11–14].

The key aspect of our analysis is the phase description of the dynamics [15]. With regard to biological oscillators, the idea of the phase description goes back to Winfree (1967) who motivated it by the observation that the oscillators should be weakly coupled so that no oscillator is ever perturbed far away from its limit cycle and therefore amplitudes could be considered as fixed [16].

Kuramoto (1975,1984) simplified the Winfree model by certain methods of perturbation and averaging [17, 18]. The Kuramoto model has been shown to be a very successful approach to the problem of synchronization [19]. Due to its simplicity the Kuramoto model is analytically tractable. We take advantage of the simplicity to the greatest extent, but at the same time we are determined to make the model more realistic, in particular with regard to neural networks. Therefore, we add two features: (i) we consider complex networks instead of all-to-all connectivity and (ii) we study noise in the phase model. The first feature takes account of the fact that many real-world networks, such as neural systems, are complex networks “par excellence” [20], while the second feature incorporates experimentally observed stochastic processes, such as the random synaptic inputs from other neurons [15].

---

\*Electronic address: sonne@physik.hu-berlin.de

For an ensemble of Kuramoto oscillators, both features have been considered separately in the literature: complex networks in [21–23] and noise in [24–26]. For an overview on nonlinear dynamics in complex networks we recommend [27–30] and for an overview on the Kuramoto model we further recommend [31, 32].

Referring to [22], we apply an approximation technique, in which we focus on the degrees of the nodes, i.e. the sums of the weights of connections leading to and emanating from a node. The degree distribution could be given “a priori” and then defines the network or it is determined by counting the frequencies of the edges and their weights for every node of the large network under consideration.

As a result of the approximation, the complex network is replaced by an all-to-all coupled one with weighted edges, which mimics the original complex structure. This procedure originates a mean-field like description that enables us to derive both the effective Langevin equation for a single oscillator inside the random network and the corresponding nonlinear Fokker-Planck equation (FPE). Moreover, the latter gives us the possibility to calculate the critical coupling strength that marks the onset of synchronization in the network.

The work is organized as follows. In section II we present our extended Kuramoto model and in section III we explain the approximation technique. In section IV we derive the nonlinear FPE and in V the critical coupling strength. This result is compared with numerical simulations for the synchronization on a small word network (section VI). In the last section VII we give concluding remarks.

## II. CONCEPTION OF OUR MODEL

We refer to the original Kuramoto model [17, 18] in the following way:

$$\dot{\phi}_i(t) = \omega_i + \frac{\varkappa}{N} \sum_{j=1}^N A_{ij} \sin(\phi_j(t) - \phi_i(t)) + \xi_i(t), \quad i = 1, \dots, N, \quad (1)$$

with the phase  $\phi_i(t)$  of oscillator  $i$  at time  $t$  and natural frequencies  $\omega_i$  drawn from a frequency distribution  $g(\omega)$  that is assumed to be symmetric with respect to the single maximum at frequency  $\omega = 0$  (due to the rotational symmetry in the model the maximum can be located like this). This assumption is also made in the original Kuramoto model. The coupling strength is denoted by  $\varkappa$  and  $A_{ij}$  are the elements of the adjacency matrix. They are nonnegative real numbers, which weight the corresponding couplings in particular, if  $A_{ij} = 0$ , then nodes  $i$  and  $j$  are not connected. The adjacency matrix gives the individual degrees:

$$k_i = \sum_{j=1}^N A_{ij}, \quad i = 1, \dots, N, \quad (2)$$

$k_i > 0$  by definition. Tracking the individual degrees of all the nodes leads to a degree distribution  $P(k)$  of the network under consideration. Remember that the indegree or the outdegree of node  $i$  are defined as the sum of the weights of edges into or emanating from node  $i$ , respectively [33]. Since we consider undirected networks, the adjacency matrix is symmetric and the indegrees are equal to the outdegrees. Hence, we refer only to the degree  $k_i > 0$  of node  $i$ .

The division by  $N$  in the coupling term of Eq. (1) is not always the correct normalization for complex networks, because it might not lead necessarily to an intensive coupling term. That is

the case, if the adjacency matrix does not scale with the system size. Then one has to take the maximum degree instead [30].

The functions  $\xi_i(t)$ ,  $i = 1, \dots, N$ , stand for sources of independent white noise processes that satisfy

$$\langle \xi_i(t) \rangle = 0, \quad (3)$$

$$\langle \xi_i(t) \xi_j(t') \rangle = 2D \delta_{ij} \delta(t - t'). \quad (4)$$

The single parameter  $D$  scales the noise intensity and is nonnegative. The angular brackets denote an average over different realizations of the noise.

### III. APPROXIMATION TECHNIQUE

The idea is to adopt a combinatorial point of view in order to mimic the complex network by a weighted fully connected network with a new adjacency matrix  $\tilde{A}_{ij}$  which should resemble the original structure defined by the given set of degrees  $k_i$ . We require that the approximating weights  $\tilde{A}_{ij}$  conserve the degrees of the original network (cf. Eq. (2)), i.e.

$$k_i \stackrel{!}{=} \sum_{j=1}^N \tilde{A}_{ij} \quad \text{and} \quad k_j \stackrel{!}{=} \sum_{i=1}^N \tilde{A}_{ij}, \quad (5)$$

where we assume again an undirected network. Eq. (5) also means that the new matrix scales in the same way as the old one, if the system size is changed.

To construct the approximating weight between nodes  $i$  and  $j$ , we assume that  $\tilde{A}_{ij}$  is proportional both to the degree  $k_i$  of the  $i$ -th node and the ratio between the degree  $k_j$  of the  $j$ -th node and the total number of all degrees in the network:

$$\tilde{A}_{ij} = k_i \frac{k_j}{\sum_{l=1}^N k_l}. \quad (6)$$

Obviously, it defines a symmetric matrix since the same expression is found using the same arguments for the weight of the edge connecting the  $j$ -th with the  $i$ -th node. It is easy to see that the new matrix conserves the local degree structure as required in Eq. (5) and the scaling of the adjacency matrix. We illustrate our approximation in Fig. 1.

Inserting Eq. (6) into Eq. (1) yields

$$\dot{\phi}_i(t) = \omega_i + \frac{\varkappa}{N} \frac{k_i}{\sum_{l=1}^N k_l} \sum_{j=1}^N k_j \sin(\phi_j(t) - \phi_i(t)) + \xi_i(t), \quad i = 1, \dots, N. \quad (7)$$

This is the approximative form of our model, which appears to be analytically tractable. For this purpose, we define the order parameter  $r(t)$  of the phase dynamics weighted according to the degrees of the current network [22]:

$$r(t) e^{i\Theta(t)} := \frac{\sum_{j=1}^N k_j e^{i\phi_j(t)}}{\sum_{j=1}^N k_j}. \quad (8)$$

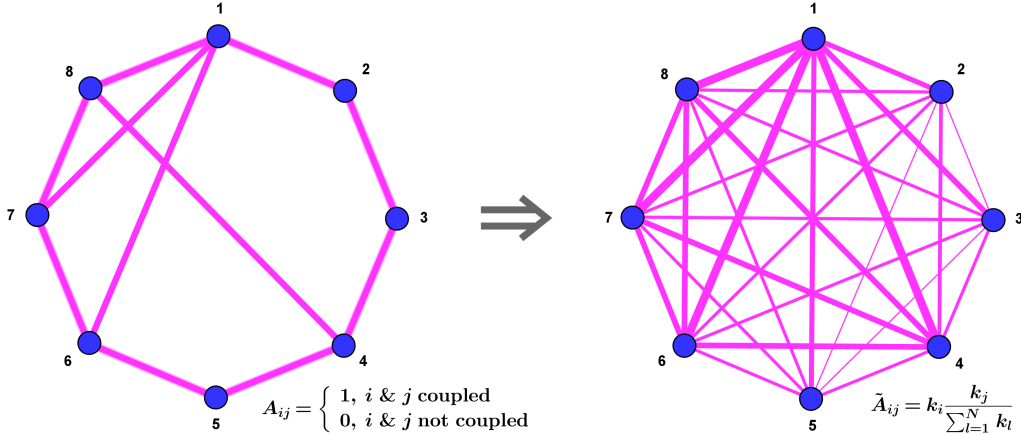


FIG. 1: (Color online) The effect of our approximation on an unweighted ring network of eight symmetrically coupled oscillators. On the left-hand side the original complex network is shown and on the right-hand side the approximate network is shown, where the thickness of the edges is chosen approximately proportional to the coupling strength. For reasons of clarity, self-coupling is not visualized.

By multiplying this equation by  $e^{-i\phi_i(t)}$  and by considering only the imaginary parts, we can rewrite Eq. (7) as an effective one-oscillator description, where the common time-dependent phase  $\Theta(t)$  and amplitude  $r(t)$  are averaged over all the nodes according to Eq. (8):

$$\dot{\phi}_i(t) = \omega_i + r(t) \kappa \frac{k_i}{N} \sin(\Theta(t) - \phi_i(t)) + \xi_i(t), \quad i = 1, \dots, N. \quad (9)$$

In other words, our approximation is equivalent to a mean field approximation with the mean field amplitude  $r(t)$  and phase  $\Theta(t)$  defined in Eq. (8). We emphasize that such an averaging requires a coarse grained statistical approach to all the nodes of the network. Each of the  $N$  oscillators are coupled to the mean field with a characteristic strength, which is proportional to the individual degree  $k_i$  given due to a common distribution. For this reason we refer to the "weighted mean field", which makes sense if the initial conditions of each oscillator have an identical distribution. Despite that Eq. (9) differs for every oscillator, later on, we will have to self-consistently average the present  $k_i$  and  $\omega_i$  over the common distributions for all nodes.

#### IV. DERIVATION OF THE NONLINEAR FOKKER-PLANCK EQUATION

The solution of the system of  $N$  coupled Langevin equations in Eq. (7) is a Markov process. It can also be formulated by the help of the transition probability  $\mathcal{P}(\phi, t | \phi^0, t^0; \omega, \mathbf{k})$  that describes the evolution of the phases from time  $t^0$  to time  $t > t^0$ . Therein, respectively the vector  $\phi = (\phi_1, \dots, \phi_N)$  contains the phases of the  $N$  oscillators at time  $t$  and  $\phi^0 = (\phi_1^0, \dots, \phi_N^0)$  at initial time  $t^0$ . The vectors  $\omega = (\omega_1, \dots, \omega_N)$  and  $\mathbf{k} = (k_1, \dots, k_N)$  contain the natural frequencies of the oscillators and the degrees of all the nodes in the network, respectively. The individual frequencies  $\omega$  and degrees  $\mathbf{k}$  are initially chosen at time  $t = t^0$  and they stay fixed during the whole evolution. We also assume that the initial phases  $\phi_i^0$  are identically and independently distributed.

The transition probability  $\mathcal{P}(\phi, t | \phi^0, t^0; \omega, \mathbf{k})$  for  $N$  oscillators satisfies a linear Fokker-Planck equation

$$\frac{\partial \mathcal{P}}{\partial t} = - \sum_i \frac{\partial}{\partial \phi_i} \left( \omega_i \mathcal{P} + k_i \frac{\varkappa}{N} \sum_{j=1}^N \frac{k_j}{\sum_{l=1}^N k_l} \sin(\phi_j - \phi_i) \mathcal{P} \right) + D \sum_i \frac{\partial^2 \mathcal{P}}{\partial \phi_i^2} \quad (10)$$

and is subject to the initial condition

$$\mathcal{P}(\phi, t^0 | \phi^0, t^0; \omega, \mathbf{k}) = \delta^N(\phi - \phi^0). \quad (11)$$

Bayes' theorem for the natural frequencies, degrees and the initial phases relates the conditioned and the joint probabilities as

$$\mathcal{P}(\phi, t | \phi^0, t^0; \omega, \mathbf{k}) = \frac{\mathcal{P}(\phi, t; \omega, \mathbf{k} | \phi^0, t^0) \mathcal{P}(\phi^0, t^0)}{\mathcal{P}(\phi^0, t^0; \omega, \mathbf{k})}. \quad (12)$$

The initial phases of the oscillators are supposed to be chosen independently of  $\omega$  and  $\mathbf{k}$ . Furthermore, as explained in section II, we consider separately a frequency  $g(\omega)$  and a degree distribution  $P(k)$ . Therefore, we have the joint distribution of initial phases, edges and frequencies at initial time  $t^0$  factorizing as

$$\mathcal{P}(\phi^0, t^0; \omega, \mathbf{k}) = \prod_{i=1}^N g(\omega_i) P(k_i) \mathcal{P}(\phi_i^0, t^0). \quad (13)$$

The joint distribution at a later time  $t$  becomes independent of the initial distribution by integration over the initial phases:

$$\mathcal{P}(\phi, t; \omega, \mathbf{k}) = \prod_{i=1}^N g(\omega_i) P(k_i) \cdot \int d\phi_i^0 \mathcal{P}(\phi, t | \phi^0, t^0; \omega, \mathbf{k}) \mathcal{P}(\phi_i^0, t^0). \quad (14)$$

Again, we aim at reducing the description to an effective one-oscillator picture. As does the transition probability, the distribution Eq. (14) obeys the FPE (10). A reduced joint distribution  $\rho_n$  with  $n < N$  for  $n$  phases with frequencies  $\omega_1 \dots \omega_n$  and degrees  $k_1, \dots, k_n$ , in a system of  $N$  statistically identical oscillators, is defined in the usual way [34]:

$$\begin{aligned} \rho_n(\phi_1, \dots, \phi_n, t; \omega_1, \dots, \omega_n, k_1, \dots, k_n) \\ := \int d\phi_{n+1} \dots d\phi_N \int d\omega_{n+1} \dots d\omega_N \int dk_{n+1} \dots dk_N \mathcal{P}(\phi, t; \omega, \mathbf{k}). \end{aligned} \quad (15)$$

For the important case of a single oscillator  $n = 1$  imbedded in the network, we integrate Eq. (10) over the remaining  $N - 1$  phases  $(\phi_2, \dots, \phi_N)$ , frequencies  $(\omega_2, \dots, \omega_N)$  and degrees  $(k_2, \dots, k_N)$ :

$$\begin{aligned} \frac{\partial \rho_1}{\partial t} = - \frac{\partial}{\partial \phi_1} \omega_1 \rho_1 + D \frac{\partial^2 \rho_1}{\partial \phi_1^2} - \\ - \frac{\partial}{\partial \phi_1} \left[ \frac{\varkappa k_1 (N-1)}{N \sum_l k_l} \int d\phi_2 \int d\omega_2 \int dk_2 \sin(\phi_2 - \phi_1) k_2 \rho_2(\phi_1, \phi_2, t; \omega_1, \omega_2, k_1, k_2) \right], \end{aligned} \quad (16)$$

where we use identity of all the oscillators in the statistical sense. As a result the binary interaction of the phase oscillators looks in the usual way and relates hierarchically to reduced probabilities

with a larger number  $n > 2$ . However, the interaction appears as averaged over the frequency and the degree distribution.

In the thermodynamic limit  $N \rightarrow \infty$  the ratio  $(N - 1)/N$  becomes unity and the correlation of phases between any two oscillators can be discarded [34] due to the mean-field interaction (cf. Eq. (9)). It might be derived in a completely rigorous way, for instance, by the help of path integral methods as in [32]. We continue with the decoupling

$$\rho_2(\phi_1, \phi_2, t; \omega_1, \omega_2, k_1, k_2) \equiv \rho_1(\phi_1, t; \omega_1, k_1) \rho_1(\phi_2, t; \omega_2, k_2) . \quad (17)$$

As a consequence we obtain an autonomous nonlinear equation for the one-oscillator probability density  $\rho_1$ :

$$\begin{aligned} \frac{\partial \rho_1(\phi_1, \omega_1, k_1)}{\partial t} &= -\frac{\partial}{\partial \phi_1} \omega_1 \rho_1 + D \frac{\partial^2 \rho_1}{\partial \phi_1^2} - \\ &- \frac{\partial}{\partial \phi_1} \rho_1 \left[ \frac{\varkappa}{N} \frac{k_1}{\langle k \rangle} \int d\phi_2 \int d\omega_2 \int dk_2 \sin(\phi_2 - \phi_1) k_2 \rho_1(\phi_2, t; \omega_2, k_2) \right] . \end{aligned} \quad (18)$$

We return to the conditional probability density

$$\rho_1(\phi_1, t | \omega_1, k_1) = \frac{\rho_1(\phi_1, t; \omega_1, k_1)}{g(\omega_1) P(k_1)} , \quad (19)$$

and get eventually a nonlinear Fokker-Planck equation:

$$\frac{\partial \rho_1(\phi_1, t | \omega_1, k_1)}{\partial t} = -\frac{\partial}{\partial \phi_1} [v(\phi_1, t) \rho_1(\phi_1, t | \omega_1, k_1)] + D \frac{\partial^2 \rho_1(\phi_1, t | \omega_1, k_1)}{\partial \phi_1^2} . \quad (20)$$

Therein the mean increment of the phase per unit time reads

$$v(\phi_1, t) = \omega_1 + r \tilde{\varkappa} k_1 \sin(\Theta - \phi_1) . \quad (21)$$

It depends on the density via the order parameter  $\rho_1(\phi_1, t | \omega_1, k_1)$

$$r e^{i\Theta} = \frac{1}{\langle k \rangle} \int_0^{2\pi} d\phi_2 \int_{-\infty}^{+\infty} d\omega_2 \int_m^{\infty} dk_2 e^{i\phi_2} \rho_1(\phi_2, t | \omega_2, k_2) k_2 P(k_2) g(\omega_2) . \quad (22)$$

Here  $\tilde{\varkappa} := \varkappa/N$  and  $m \geq 1$  is the lowest possible degree in our network. Eq. (20) is again an effective one-oscillator description as Eq. (9). Both descriptions are equivalent for all possible pairs  $\omega_i$  and  $k_i$ . We remark that our expressions are reminiscent of the equations in the work of Ichinomiya [22], who considers a random network without noise. We also note that the conditional probability distribution density  $\rho_1(\phi_1, t | \omega_1, k_1)$  in Eq. (19) is averaged over the initial conditions. If one would formulate the theory for the transition probability  $\rho_1(\phi_1, t | \phi^0, t^0, \omega_1, k_1)$  the nonlinear FPE (20) would be the same. A difference would occur in the definition of the order parameter, where one has to remember that the definition (22) includes the average over the initial conditions as it was performed in Eq. (13).

## V. THE CRITICAL COUPLING STRENGTH

To underline the statistical identity of the oscillators in the one-oscillator description, we omit the indices and proceed with variables  $\phi, \omega, k$ . Taking into account the normalization condition

$$\int_0^{2\pi} \rho(\phi, t | \omega, k) d\phi = 1 , \quad \forall \omega, k, t , \quad (23)$$

the completely asynchronous stationary state is given by

$$\rho_0(\phi|\omega, k) = \frac{1}{2\pi} = \text{const.}, \quad \forall \omega, k, t \quad (24)$$

with order parameter  $r = r_0 = 0$  and undefined phase. It is easy to see that  $\rho_0$  is at least one of the possible asymptotic solutions of the nonlinear FPE (22).

In the following, we will perform a linear stability analysis of this incoherent solution. In doing so, we refer to the work of Strogatz and Mirollo [25], who investigate the linear stability of the incoherent state for an unweighted all-to-all connectivity. The critical condition, where the incoherent solution loses its stability, is equivalent to the onset of synchronization we are searching for. To start with, we consider the evolution of a small perturbation of the incoherent state:

$$\rho(\phi, t|\omega, k) = \frac{1}{2\pi} + \epsilon \delta\rho(\phi, t|\omega, k), \quad \epsilon \ll 1. \quad (25)$$

The normalization condition (23) implies

$$\epsilon \int_0^{2\pi} \delta\rho(\phi, t|\omega, k) d\phi = 0 \quad \forall \omega, k, t, \quad (26)$$

so  $\delta\rho(\phi, t|\omega, k)$  is  $2\pi$ -periodic in  $\phi$ . Now we substitute Eq. (25) into Eq. (20),

$$\epsilon \frac{\partial \delta\rho}{\partial t} = -\frac{\partial}{\partial \phi} \left[ \left( \frac{1}{2\pi} + \epsilon \delta\rho \right) v \right] + \epsilon D \frac{\partial^2 \delta\rho}{\partial \phi^2}. \quad (27)$$

The amplitude becomes  $r(t) = \epsilon \delta r(t)$ , where  $\delta r(t)$  is given by substituting  $\rho$  by  $\delta\rho$  in Eq. (22). The FPE (20) linearized in the lowest order in  $\epsilon$  then reads

$$\frac{\partial \delta\rho}{\partial t} = -\omega \frac{\partial \delta\rho}{\partial \phi} + \frac{\tilde{\alpha} k}{2\pi} \delta r \cos(\Theta - \phi) + D \frac{\partial^2 \delta\rho}{\partial \phi^2}. \quad (28)$$

Since  $\delta\rho$  is a real number and  $2\pi$ -periodic in  $\phi$  (cf. Eq. (26)), it may be expanded as

$$\delta\rho(\phi, t|\omega, k) = \frac{1}{2\pi} \sum_{l=1}^{\infty} \{ c_l(t|\omega, k) e^{il\phi} + c_l^*(t|\omega, k) e^{-il\phi} \}. \quad (29)$$

Due to Eq. (26),  $c_0(t|\omega, k)$  vanishes. The first nonvanishing coefficients, which constitute the so-called fundamental mode, determine the deviations of the mean field in first order of small  $\epsilon$ :

$$\delta r e^{i\Theta} = \frac{1}{\langle k \rangle} \int_{-\infty}^{+\infty} d\omega' \int_m^{\infty} dk' c_1^*(t|\omega', k') k' P(k') g(\omega'). \quad (30)$$

In order that the incoherent state becomes unstable and a synchronization process starts,  $c_1(t|\omega, k)$  has to grow, so that as a consequence the order parameter  $r(t)$  grows as well.

Multiplication of the last equation by  $e^{-i\phi}$  and considering only the real parts, yields

$$\delta r \cos(\Theta - \phi) = \frac{1}{2\langle k \rangle} \left( \int_{-\infty}^{+\infty} d\omega' \int_m^{\infty} dk' c_1(t|\omega', k') k' P(k') g(\omega') \right) e^{i\phi} + \text{c. c.} \quad (31)$$

Now we insert Eqs. (29)-(31) into Eq. (28) and consider only the coefficients with  $e^{i\phi}$ . Afterwards, one finds the evolution equation for the fundamental mode  $c_1(t|\omega, k)$ :

$$\frac{\partial c_1}{\partial t} = -(D + i\omega)c_1 + \frac{\tilde{\varepsilon}k}{2\langle k \rangle} \int_{-\infty}^{+\infty} d\omega' \int_m^{\infty} dk' c_1(t|\omega', k') k' P(k') g(\omega'). \quad (32)$$

Since this is a partial differential equation without mixed derivatives, we make a separation ansatz:

$$c_1(t|\omega, k) = b(\omega, k)e^{\lambda t}, \quad \lambda \in \mathbb{C}. \quad (33)$$

So we obtain

$$\lambda b = -(D + i\omega)b + \frac{\tilde{\varepsilon}k}{2\langle k \rangle} \int_{-\infty}^{+\infty} d\omega' \int_m^{\infty} dk' b(\omega', k') k' P(k') g(\omega'). \quad (34)$$

The right-hand side is a linear transformation and it can be shown that we only have to calculate its point spectrum in order to obtain the critical coupling strength [25].

The second term on the right-hand side of Eq. (34) equals the degree  $k$  times a constant which we call  $B$  in the following, so that  $b(\omega, k)$  is given by

$$b(\omega, k) = \frac{B \cdot k}{\lambda + D + i\omega}. \quad (35)$$

Hence, we can set up the following self-consistent equation:

$$B = \frac{\tilde{\varepsilon} \langle k^2 \rangle}{2 \langle k \rangle} \int_{-\infty}^{+\infty} \frac{B}{\lambda + D + i\omega'} g(\omega') d\omega'. \quad (36)$$

This relation holds, if all the oscillators are identical in the statistical sense, see section IV. The solution  $B = 0$  is not allowed, because otherwise  $b(\omega, k)$  and as a consequence  $c_1(t|\omega, k)$  would vanish.  $c_1(t|\omega, k) = 0$  however is not considered as an eigenfunction (it is a trivial solution). So  $B$  is canceled out and we get

$$1 = \frac{\tilde{\varepsilon} \langle k^2 \rangle}{2 \langle k \rangle} \int_{-\infty}^{+\infty} \frac{g(\omega')}{\lambda + D + i\omega'} d\omega'. \quad (37)$$

On the analogy of the proof in [35], one can show that there exists only one solution for  $\lambda$  and that it has to be a real number. The proof makes use of the assumption that  $g(\omega)$  is symmetric with respect to the single maximum (cf. section II).

In summary the eigenvalue  $\lambda$  is given by

$$1 = \frac{\tilde{\varepsilon} \langle k^2 \rangle}{2 \langle k \rangle} \int_{-\infty}^{+\infty} \frac{\lambda + D}{(\lambda + D)^2 + \omega'^2} g(\omega') d\omega'. \quad (38)$$

Note that this equation can only be fulfilled if  $\lambda > -D$ , because otherwise the right-hand side would be nonpositive. Thus, the eigenvalue  $\lambda$  is nonnegative and the incoherent solution cannot be linearly stable, if the noise intensity vanishes.

At the critical condition  $\lambda = \lambda_c = 0$  the incoherent solution loses its stability: if  $\lambda > 0$  the fundamental mode  $c_1$  of the perturbation  $\delta\rho$  of the incoherent solution is linearly unstable. It



grows exponentially with time  $\sim e^{\lambda t}$  and so does the order parameter  $r(t)$  (cf. Eq. (30)). Hence, the critical coupling strength  $\varkappa_c$  for the onset of synchronization reads

$$\varkappa_c = 2N \frac{\langle k \rangle}{\langle k^2 \rangle} \left[ \int_{-\infty}^{+\infty} \frac{D}{D^2 + \omega'^2} g(\omega') d\omega' \right]^{-1}. \quad (39)$$

We emphasize that this equation is not valid in the noise-free case, where one has to take the limit  $\lambda \rightarrow 0^+$  in Eq. (38) with  $D = 0$ , by which previous results can be reproduced [22, 23] (compare Tab. I).

It is interesting to see that the critical coupling strength  $\varkappa_c$  can be written as a product of two functionals. The first one maps the degree distribution  $P(k)$  to a real number via the first two moments,

$$f_{\text{top}}[P] := N \frac{\langle k \rangle}{\langle k^2 \rangle}. \quad (40)$$

We call this one the "topology functional". The second one maps the frequency distribution  $g(\omega)$  to a real number via an integral that depends on the noise intensity  $D$ ,

$$f_{\text{div}}(D)[g] := 2 \left[ \int_{-\infty}^{+\infty} \frac{D}{D^2 + \omega'^2} g(\omega') d\omega' \right]^{-1}. \quad (41)$$

We call this one the "diversity functional". In short:

$$\varkappa_c = f_{\text{top}}[P] \cdot f_{\text{div}}(D)[g]. \quad (42)$$

The factorization results partly from the separate distributions for the degrees  $\mathbf{k}$  and the natural frequencies  $\omega$ . In [36] we investigate the effects of correlations between the two quantities.

## VI. APPLICATION TO A DENSE SMALL-WORLD NETWORK MODEL

In this section we test the analytical expression for the critical coupling strength as a function of diversity, noise and network topology for local ring-like networks, where random shortcuts to other nodes will be established. For this purpose, we compare the analytical result with numerical simulations of networks with different size  $N$ .

### A. Derivation of the Topology Function

First, we specify our dense small-world network model. According to the definition in [37], in dense networks of  $N$  nodes the total number of edges scales with  $N^2$ . Our dense small-world networks are constructed as follows. Each oscillator is coupled to its  $K$  next neighbors in both directions of the ring network and  $K$  is given by

$$K = \left\lfloor \frac{\alpha}{2}(N - 1) \right\rfloor, \quad 0 \leq \alpha \leq 1. \quad (43)$$

Here the intensive variable  $\alpha$  gives the fraction of all nodes which are coupled to a single one on the ring.  $\alpha = 0$  stands for uncoupled nodes, whereas in case of  $\alpha = 1$  the network is fully connected.

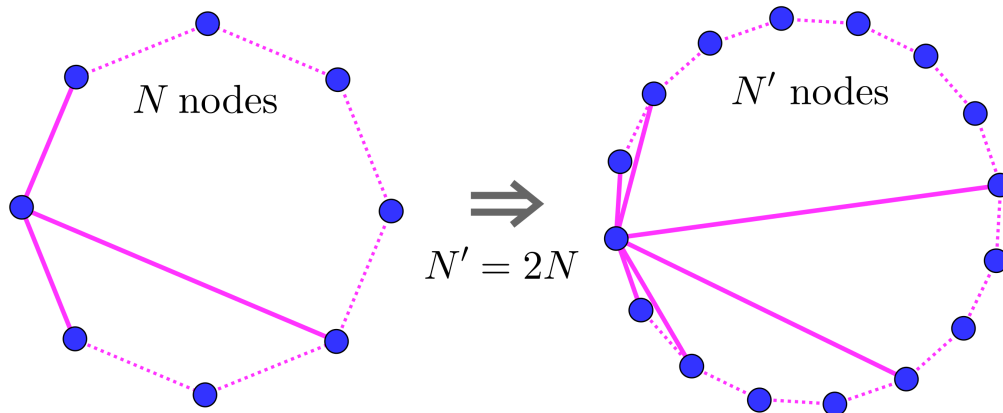


FIG. 2: (Color online) Visualization of a dense small-world network model. If the system size  $N$  is duplicated, the average number of connections is duplicated as well. The figure shows one marked node in the network.

We underline that the variance of  $\alpha$  vanishes. The floor function  $\lfloor \cdot \rfloor$  gives the greatest integer less than or equal to its argument. So far we obtain a regular network and due to self-coupling, the fixed degree in such regular networks is  $2K + 1$ . The corresponding degree distribution is equal to the Kronecker symbol

$$P_{\text{local}}(k) = \delta_{k, 2K+1} \quad (44)$$

In our simulations we choose  $\alpha = 0.05$ . Hence, 2.5 percent of possible edges are local regular connections.

Besides these  $(2K + 1) \cdot N$  next neighbor couplings we introduce shortcuts: each oscillator is coupled to the remaining other  $N - 2K - 1$  ones with a certain probability  $p$  (see Fig. 2 for illustration). The case  $p = 1$  leads to all-to-all connectivity in contrast to the rewiring probability in the original sparse small-world network model [38, 39]. The procedure of adding shortcuts can be seen as a Bernoulli experiment with probability  $p$  of success [27–29], so that the degree distribution  $P(k)$  is given by the following binomial distribution:

$$P(k) = \binom{N - 2K - 1}{k - 2K - 1} p^{k - 2K - 1} [1 - p]^{N - k}, \quad k > 2K. \quad (45)$$

Note that the minimum degree  $k = 2K + 1$  corresponds to Eq. (44). The first moment equals

$$\langle k \rangle = 2K + 1 + (N - 2K - 1)p \approx (N - 1)(\alpha + p - \alpha p) + 1. \quad (46)$$

In the last step we have used Eq. (43) by neglecting the floor function as an approximation. For large  $N$  the latter expression approaches  $\langle k \rangle \approx N(\alpha + p - \alpha p)$ .

By simple substitutions one finds the second moment

$$\langle k^2 \rangle = (\langle k \rangle + 2K + 1)^2 + \langle k \rangle(1 - p), \quad (47)$$

where the second item equals the variance of  $k$  in the binomial distribution due to the randomness of the numbers of shortcuts. It scales only linearly with the system size, whereas the first item

grows with  $N^2$ . Thus, for large systems the difference between the nonrandom number of local connections and the number of shortcuts disappears, because the variability of the shortcuts does not count for large  $N$ . The second moment becomes symmetric in  $\alpha$  and  $p$ :

$$\langle k^2 \rangle \approx N^2 \left( (p + \alpha)^2 + \alpha p (\alpha p - 2\alpha - 2p) \right) . \quad (48)$$

Hence, the topology function (cf. Eq. (40)) for large  $N$  results in

$$f_{\text{top}}(p, \alpha)|_{N \gg 1} \approx \frac{\alpha + p - \alpha p}{p^2 + \alpha^2 + \alpha^2 p^2 + 2(\alpha p - \alpha p^2 - \alpha^2 p)} . \quad (49)$$

We obtain as limiting cases

$$f_{\text{top}}(p, \alpha)|_{N \gg 1} \approx \begin{cases} \frac{1}{\alpha} + \frac{\alpha-1}{\alpha^2} p + O(p^2), & p \ll 1, \\ 2 - \alpha + (\alpha - 1)p + O(p^2), & p \lesssim 1. \end{cases} \quad (50)$$

Due to the symmetry, we obtain qualitatively the same for  $\alpha \ll 1$  and  $\alpha \lesssim 1$ , but with  $p$  and  $\alpha$  being interchanged. As expected, the topology function tends to unity for  $p \rightarrow 1$  or  $\alpha \rightarrow 1$ , because in both cases the network becomes fully connected.

In Fig. 3 the dependence of the topology function on  $\alpha$  and  $p$  is depicted. Discrepancies between numerical calculations and theory in the right panel are due to the fact that the number of coupled next neighbors is, of course, an integer. Rounding off in Eq. (43) leads to noticeable steps in  $f_{\text{top}}(p, \alpha)$  for smaller  $N$ .

We emphasize that by the help of Eqs. (46) and (47), one can find the exact expression for the topology function for arbitrary system sizes. Since it is a rather lengthy expression, we skip it in the text but we will use it in Fig. 3. Moreover, as can be seen in Fig. 3, a system size  $N$  of the order  $O(100)$  is sufficient to obtain a dynamical behavior that is comparable with the thermodynamic limit. Further, the critical coupling strength  $\varkappa_c$  has been derived in the thermodynamic limit (see Eq. (42)). For this reason it is only consistent to calculate the topology function in the limit  $N \rightarrow \infty$  as well.

## B. Comparison of the Critical Coupling Strength; Simulations vs. Theory

In our simulations, the stochastic differential equations (1) are integrated up to  $t = 600$  with time step  $h = 0.05$  by using the Heun scheme [40]. The periods of the oscillators are  $T \sim O(10)$ , so our integrations cover  $O(10)$  periods. Moreover, in order to calculate statistical equilibria, we discard the data up to  $t = 200$ , by which transient effects are safely avoided. The statistical equilibria are further calculated as averages over at least 100 different network realizations. We emphasize that all the different network configurations do not differ only in the configuration of the connections, but the oscillators on the network differ as well: all the natural frequencies and the initial values of the phases change from one configuration to another one.

Hong, Choi and Kim (2002) consider the Kuramoto model without noise on a small-world network, which is constructed according to the Watts-Strogatz model [38], where shortcuts are the result of rewiring the edges of the initial regular network with a certain probability  $p$  [21]. They calculate the order parameter averaged over time  $\langle \dots \rangle$  and network realizations  $[\dots]$  and their finding is that it has the following scaling form in the thermodynamic limit  $N \rightarrow \infty$ :

$$\text{sync} := \left[ \left\langle \left| \frac{1}{N} \sum_{j=1}^N e^{i\phi_j} \right| \right\rangle \right] = N^{-\frac{\beta}{\nu}} F \left[ (\varkappa - \varkappa_c) N^{\frac{1}{\nu}} \right] , \quad (51)$$

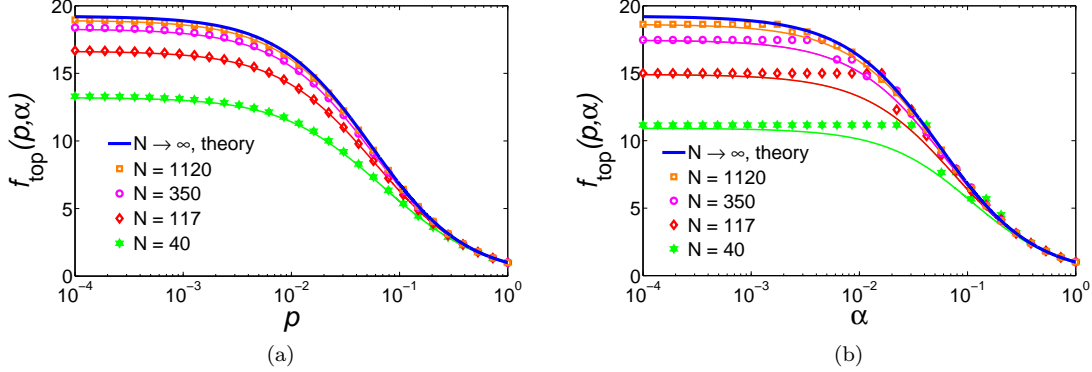


FIG. 3: (Color online) Dependency of the topology function on the system size  $N$ : Solid lines are given by the theory. The thick line corresponds to the thermodynamic limit and slight lines are calculated according to Eqs. (46) and (47) for smaller systems. Markers show results of numerical calculations for indicated system sizes.

where  $F[.]$  is some scaling function. In particular it is found that  $\beta$  and  $\nu$  have the same values as in the globally connected network, namely  $\beta \approx \frac{1}{2}$  and  $\nu \approx 2$ .

The findings in [21] propose a finite-size scaling analysis to calculate the critical coupling strength, because at  $\varkappa = \varkappa_c$  the function  $F[.]$  is independent of the system size  $N$ . By plotting  $\text{sync} \cdot N^{\frac{1}{4}}$  as a function of  $\varkappa$  for various network sizes  $N$ , we can measure the critical coupling strength  $\varkappa_c$  as a well-defined intersection point, see Fig. 4.

In order to compare the theory, expressed by the critical coupling strength (Eq. (42)), with simulations on the proposed dense small-world networks, we use as topology functional the approximation for large systems (cf. Eq. (49)).

In the following we further consider a Gaussian frequency distribution  $g_{\text{gauss}}(\omega)$  with vanishing mean and standard deviation  $\sigma$ . Then for the diversity functional (41) the expression

$$f_{\text{div}}(D)[g_{\text{gauss}}] = 2\sqrt{\frac{2}{\pi}}\sigma \left[ 1 - \Phi\left(\frac{D}{\sqrt{2}\sigma}\right) \right]^{-1} e^{-\frac{1}{2}\frac{D^2}{\sigma^2}} \quad (52)$$

follows;  $\Phi(\cdot)$  is the error function. The formula is equivalent to the mean field expression derived in [25] by means of an eigenvalue analysis. In appendix B we summarize the limiting cases of Eq. (52) and we give a comparison with other frequency distributions.

As can be seen in Figs. 5 and 6 we obtain a satisfying agreement for the critical coupling strength  $\varkappa_c$ , regardless of whether we consider the dependencies on the topology (Fig. 5) or the dependencies on the diversity (Fig. 6).

Especially for  $p > 0.1$ ,  $\alpha > 0.1$  or  $\sigma < 0.5$  and for the dependency on the noise intensity  $D$  in general, we obtain almost a perfect agreement between theory and simulations. For smaller values of  $p$  or  $\alpha$  there is a small discrepancy, but the shape of the curves can be well reproduced.

As expected, both weaker connectivity and larger diversity impede synchronization. Compare Eq. (50) and Tab. I for a summary of the limiting cases. In particular, for  $p \rightarrow 0$  or  $\alpha \rightarrow 0$  our results suggest a saturation at the values  $\varkappa_c = \frac{f_{\text{div}}(D)[g]}{\alpha}$  or  $\varkappa_c = \frac{f_{\text{div}}(D)[g]}{p}$ , respectively.

Apparently, the weighted mean-field approximation tends to overestimate the critical coupling strength, which is counterintuitive, because the approximation corresponds to a weighted fully

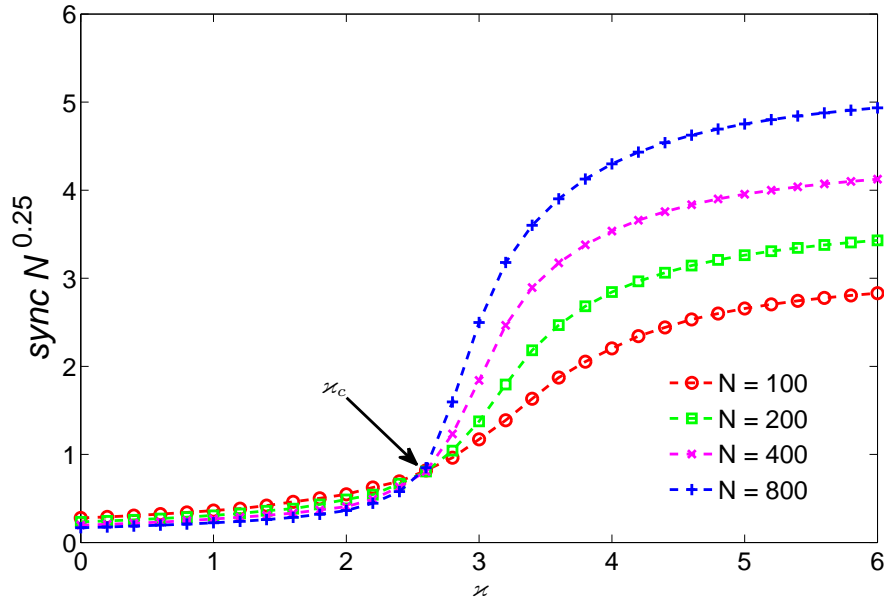


FIG. 4: (Color online) Numerical determination of critical coupling strength by plotting the order parameter  $\text{sync } N^{0.25}$  for different system sizes in dependence on the coupling strength. According to Eq. (51) the intersection of the curves indicate the critical coupling strength. Parameter values here:  $\alpha = 0.05$ ,  $p = 0.1$ ,  $D = 0.05$ ,  $\sigma = 0.02$ .

connected network and all-to-all connectivity should reduce the critical coupling strength. To see this, compare  $p = 1$  or  $\alpha = 1$  in Fig. 5, because both choices stand for all-to-all connectivity. So the coupling weights defined in Eq. (6) are able to mimic the original complexity in an overstated manner.

The disagreement for high standard deviations  $\sigma$  of the Gaussian frequency distribution seems to be analogous to the disagreement in the dependency on the topology, because in our derivation of the critical coupling strength, both the frequency distribution  $g(\omega)$  and the degree distribution  $P(k)$  are involved in averaging.

## VII. CONCLUSION

We have investigated noisy Kuramoto oscillators on undirected ring networks, whose complex structure is approximated by a weighted fully connected network. The weights are obtained by a specific combinatorial consideration of the connectivity and we have shown that this procedure leads to a weighted mean-field approximation, which enabled us to evaluate analytically the critical coupling strength  $\varkappa_c$  that marks the onset of synchronization in the network. As a result, we have found that  $\varkappa_c$  is a product of two functionals. The first one is a functional of the degree distribution and therefore depends solely on the network topology, while the second one is a functional of the

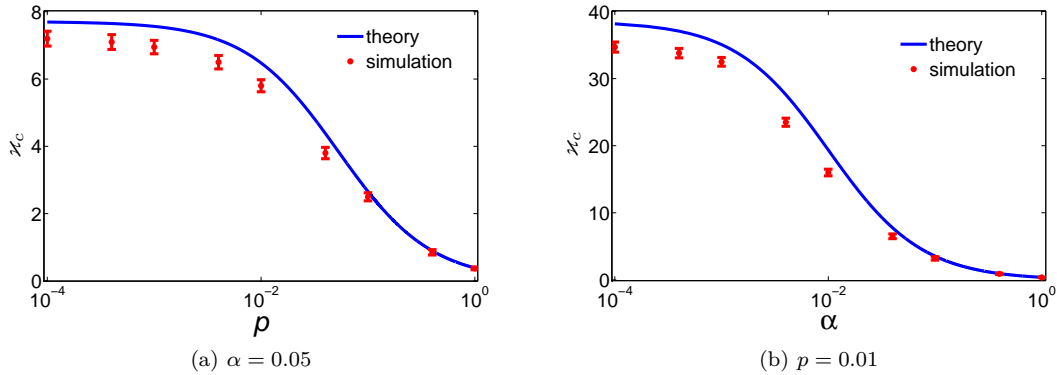


FIG. 5: (Color online) The dependencies of the critical coupling strength  $\kappa_c$  on the shortcut probability  $p$  and on the parameter  $\alpha$  for the local connections are shown. Remaining parameters:  $D = 0.05$ ,  $\sigma = 0.2$ .

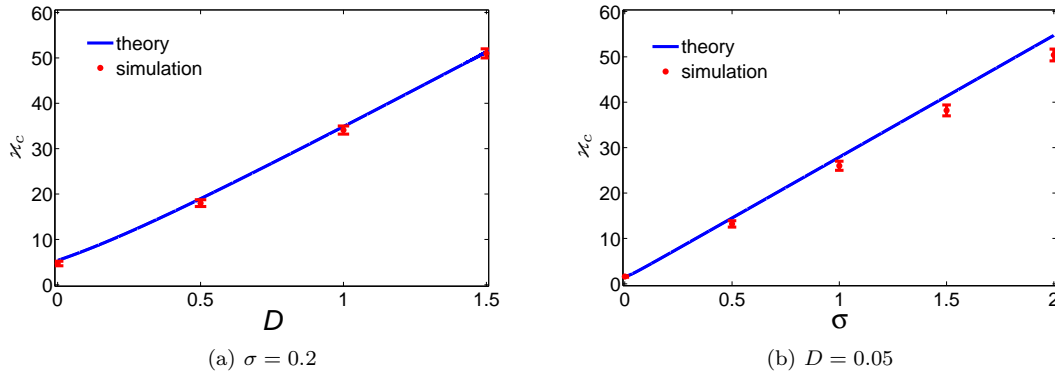


FIG. 6: (Color online) The dependencies of the critical coupling strength  $\kappa_c$  on the noise intensity  $D$  and on the diversity parameter  $\sigma$  are depicted. Remaining parameters:  $\alpha = 0.05$ ,  $p = 0.01$ .

frequency distribution and a function of the noise intensity.

As such, we have provided support for the previous separate consideration of network complexity and noise with regard to the Kuramoto model in the literature.

In order to compare the theory with simulations, we have investigated a dense small-world network model. As typical of small-world networks [39], we start with a regular network consisting only of next neighbor couplings, and then we randomly add shortcuts. In this way one can study the impact and the interplay of regular local edges and random shortcuts. We have found that in a large small-world network, regular local edges and random shortcuts play almost the same role.

Our dense small-world network model allows scaling between a locally and a globally connected network, which is well-suited for testing the mean-field approximation. In case of all-to-all connectivity the mean-field description is exact; by decreasing the connectivity we can determine the arising discrepancies between the original complexity and our estimate.

It has turned out that the analytical and the numerical results are consistent to each other in par-

ticular, finite-size scaling analysis with mean-field exponents always gives a well-defined intersection point. Hence, the extended Kuramoto model on dense small-world networks shows a mean-field synchronization transition.

Future work has to be done with regard to network complexity. For instance whether networks of higher dimension show significant qualitative differences. In particular, the problem of time-dependent coupling strengths or even time-dependent number of nodes and edges has to be tackled. A next step could also be the consideration of time delays in the coupling. Furthermore, network costs have to be taken into account, which should allow to evaluate the efficiency of a synchronization process.

### Acknowledgments

This work was supported by GRK1589/1. We acknowledge F. Sagués (Barcelona), S. Martens (Berlin) and P. K. Radtke (Berlin) for a critical reading of the manuscript.

### Appendix A: Dense Small-World Networks

Here we provide numerical evidence for the existence of dense small-world networks, see Fig. 7. In order to do this, we have to compare such dense small-world networks with random networks. However, the random network used for the comparison must not have any isolated nodes. Otherwise path length and clustering coefficient are not (well) defined. We take as an almost random network (similar to Watts and Strogatz [38]) a network generated with our model, but with a minimum amount of coupled next neighbors, so we choose  $K = 1$  or an equivalent  $\alpha$  (cf. Eq. (43)). The comparison makes sense, only if the average degree  $\langle k \rangle$  of both networks is the same, which requires choosing the following shortcut probability  $p'$  for the random network:

$$p' = \frac{2(K-1)}{N-3} + \frac{N-2K-1}{N-3}p. \quad (\text{A1})$$

$p$  is the shortcut probability used for the dense small-world network.

Having in mind the defining properties of a small-world network:  $L \gtrsim L_{\text{random}}$  and  $C \gg C_{\text{random}}$  [38], we observe small-world networks for values of  $p$  around  $10^{-3}$ . For smaller values of  $\alpha$ , i.e., fewer coupled next neighbors, the defining properties are better fulfilled. If  $\alpha$  is too large the network under consideration is no small-world network anymore.

### Appendix B: Diversity Functional for Different Frequency Distributions

In what follows, we consider the diversity functional for different frequency distributions: uniform distribution  $g_{\text{uni}}(\omega)$ , identical oscillators  $g_{\text{ident}}(\omega)$  and Lorentzian distribution  $g_{\text{lorentz}}(\omega)$ . We obtain the following expressions for the diversity functionals (cf. Eq. (41)):

$$\begin{aligned} f_{\text{div}}(D)[g_{\text{uni}}] &= 2\sqrt{3}\sigma \left[ \arctan \left( \frac{\sqrt{3}\sigma}{D} \right) \right]^{-1}, \\ f_{\text{div}}(D)[g_{\text{ident}}] &= 2D, \\ f_{\text{div}}(D)[g_{\text{lorentz}}] &= 2(D + \gamma). \end{aligned} \quad (\text{B1})$$

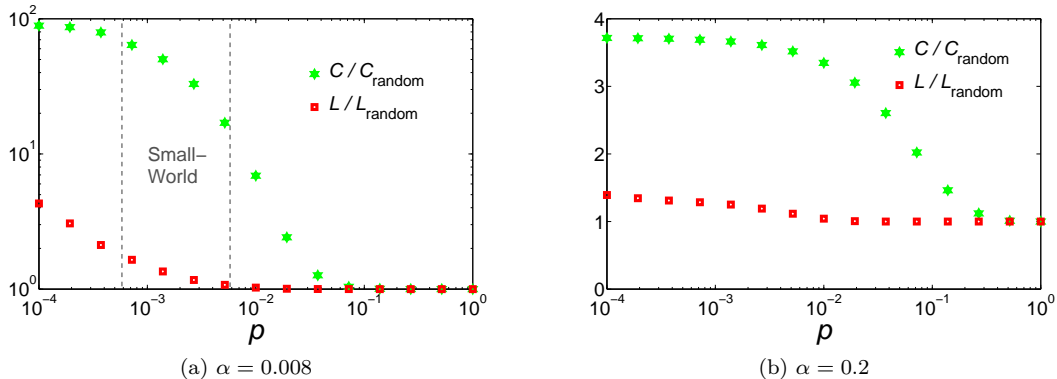


FIG. 7: (Color online) Numerically calculated average path lengths  $L$  and clustering coefficients  $C$  as a function of shortcut probability  $p$  for a network of 501 nodes. The radius of coupled next neighbors (compare Eq. (43)) equals  $K = 2$  (Fig. 7(a)) or  $K = 50$  (Fig. 7(b)), respectively. Dashed lines indicate the area, in which our model generates a small-world network.

$\sigma$  and  $\gamma$  are the standard deviation and the scale parameter, respectively, while  $D$  gives the noise intensity. In Fig. 8 the dependencies on  $D$ ,  $\sigma$  or  $\gamma$  are depicted. We observe a greater difference in the dependency on diversity than on noise. In particular, for large values of  $D$ , all the different diversity functionals show the same linear dependency on  $D$  (cf. Fig. 8(a)). In case of Gaussian, uniformly and identically distributed natural frequencies  $\omega$ , it can be shown that the diversity functional even approaches the same line for  $D \rightarrow \infty$ .

However, the above observation is not surprising, because the noise acts on the natural frequencies. So if the noise intensity  $D$  is very high, it makes almost no difference how the natural frequencies are distributed, because the diversity of the oscillators mainly comes from the random fluctuations induced by the noise.

Instead, for  $D = \text{const.}$  and increasing diversity parameter  $\sigma$  or  $\gamma$ , the different nature of the various frequency distributions manifests more and more in a different synchronizability (cf. Fig. 8(b)). Especially the comparison between the uniform and the Lorentzian distribution for the same  $\sigma$  and  $\gamma$  values is interesting. In terms of synchronizability we observe that for lower diversity the uniform frequency distribution is more favorable than the Lorentzian distribution, while for higher diversity the Lorentzian distribution is more favorable.

Of course, vanishing diversity, i.e.,  $\sigma \rightarrow 0$  or  $\gamma \rightarrow 0$ , results in identical oscillators, so that the diversity functional approaches the same value for every frequency distribution. In Tab. I we summarize these results.

LIMITING CASE	$D \ll 1$	$\sigma \ll 1$	$D \gg 1$	$\sigma \gg 1$
$f_{\text{div}}(D)[g_{\text{gauss}}]$	$2\sqrt{\frac{2}{\pi}}\sigma + \frac{4}{\pi}D + O(D^2)$	$2D + \frac{2}{D}\sigma^2 + O(\sigma^4)$	$2D + O(\frac{1}{D})$	$2\sqrt{\frac{2}{\pi}}\sigma + O(1)$
$f_{\text{div}}(D)[g_{\text{uni}}]$	$\frac{4\sqrt{3}}{\pi}\sigma + \frac{8}{\pi^2}D + O(D^2)$	$2D + \frac{2}{D}\sigma^2 + O(\sigma^4)$	$2D + O(\frac{1}{D})$	$\frac{4\sqrt{3}}{\pi}\sigma + O(1)$
$f_{\text{div}}(D)[g_{\text{ident}}]$	$2D$	$2D$	$2D$	$2D$
$f_{\text{div}}(D)[g_{\text{lorenz}}]$	$2\sigma + 2D$	$2D + 2\sigma$	$2D + O(1)$	$2\sigma + O(1)$

TABLE I: The limiting cases of the diversity functional for different frequency distributions. Here  $\sigma = \lambda$ .



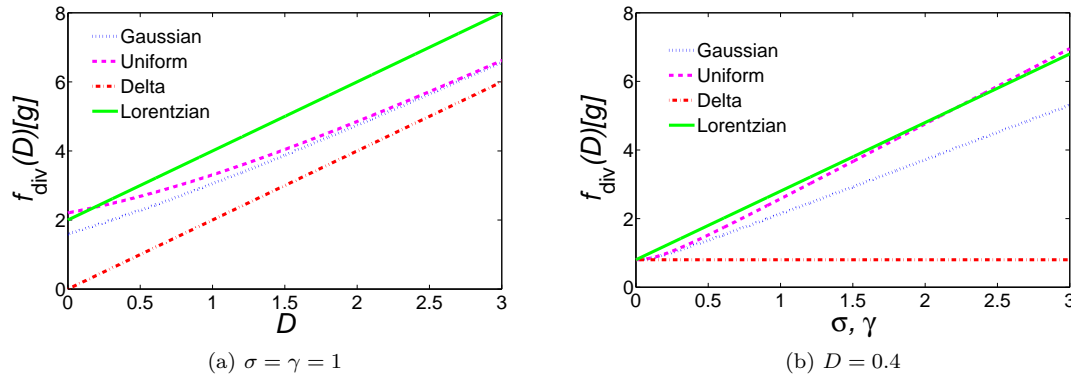


FIG. 8: (Color online) The diversity functional for different frequency distributions as a function of noise intensity  $D$ , standard deviation  $\sigma$  or scale parameter  $\gamma$ .

- 
- [1] R. Roy and Jr. K. S. Thornburg. *Phys. Rev. Lett.*, 72(13):2009–2012, 1994.
  - [2] J. Buck and E. Buck. *Scientific Am.*, 234:74–85, 1976.
  - [3] J. Dye. *J. Comp. Physiol. A*, 168(5):521–532, 1991.
  - [4] T. A. Engel, B. Helbig, D. F. Russell, L. Schimansky-Geier, and A. B. Neiman. *Phys. Rev. E*, 80(021919):1–7, 2009.
  - [5] S. Olmi, R. Livi, A. Politi, and A. Torcini. *Phys. Rev. E*, 81(046119):1–7, 2010.
  - [6] S. Luccioli and A. Politi. *Phys. Rev. Lett.*, 105(158104):1–4, 2010.
  - [7] T. Doerr, R. Denger, and W. Trautwein. *Pflügers Arch*, 413(6):599–603, 1989.
  - [8] M. K. McClintock. *Nature*, 229:244–245, 1971.
  - [9] H. C. Wilson. *Psychoneuroendocrinology*, 17(6):565–591, 1992.
  - [10] Z. Yang and J. C. Schank. *Human Nature*, 17(4):433–447, 2006.
  - [11] A. Pikovsky, M. Rosenblum, and J. Kurths. *Synchronization: A universal concept in nonlinear sciences*. Cambridge Univ. Press, U. K., 2003.
  - [12] P. Tass. *Phase Resetting in Medicine and Biology*. Springer-Verlag, Berlin, Heidelberg, New York, Tokyo, 2007.
  - [13] V. S. Anishchenko, V. Astakhov, A. Neiman, T. Vadisova, and L. Schimansky-Geier. *Nonlinear Dynamics of Chaotic and Stochastic Systems*. Springer-Verlag, Berlin, Heidelberg, New York, Tokyo, 2007.
  - [14] A. Balanov, N. Janson, D. Postnov, and O. Sosnovtseva. *Synchronization: From Simple to Complex*. Springer-Verlag, Berlin, Heidelberg, New York, Tokyo, 2010.
  - [15] B. Lindner, J. García-Ojalvo, A. Neiman, and L. Schimansky-Geier. *Physics Reports*, 392:321–424, 2004.
  - [16] A. T. Winfree. *J. Theor. Biol.*, 16:15–42, 1967.
  - [17] Y. Kuramoto. Self-entrainment of a population of coupled non-linear oscillators. In H. Araki, editor, *Lecture Notes in Physics*, volume 39, pages 420–422. Springer, New York, 1975.
  - [18] Y. Kuramoto. *Chemical Oscillations, Waves, and Turbulence*. Springer-Verlag, Berlin, Heidelberg, New York, Tokyo, 1984.
  - [19] J. Ochab and P. F. Góra. *Acta Physica Polonica B Proceedings Supplement*, 3(2):453–462, 2010.
  - [20] O. Sporns, D. R. Chialvo, M. Kaiser, and C. C. Hilgetag. *TRENDS in Cognitive Sciences*, 8(9):418–425, 2004.

- [21] H. Hong, M. Y. Choi, and B. J. Kim. *Phys. Rev. E*, 65(026139):1–5, 2002.
- [22] T. Ichinomiya. *Phys. Rev. E*, 70(026116):1–5, 2004.
- [23] J. G. Restrepo, E. Ott, and B. R. Hunt. *Phys. Rev. E*, 71(036151):1–12, 2005.
- [24] H. Sakaguchi. *Prog. Theor. Phys.*, 79(1):39–46, 1988.
- [25] S. H. Strogatz and R. E. Mirollo. *Journal of Statistical Physics*, 63(3/4):613–635, 1991.
- [26] M. A. Zaks, A. B. Neiman, S. Feistel, and L. Schimansky-Geier. *Phys. Rev. E*, 68(066206):1–9, 2003.
- [27] R. Albert and A.-L. Barabási. *Rev. Mod. Phys.*, 74(1):47–97, 2002.
- [28] M. E. J. Newman. *SIAM Review*, 45(2):167–256, 2003.
- [29] S. Boccaletti, V. Latora, Y. Moreno, M. Chavez, and D.-U. Hwang. *Physics Reports*, 424:175–308, 2006.
- [30] A. Arenas, A. Díaz-Guilera, J. Kurths, Y. Moreno, and C. Zhou. *Physics Reports*, 469:93–153, 2008.
- [31] S. H. Strogatz. *Physica D*, 143:1–20, 2000.
- [32] J. A. Acebrón, L. L. Bonilla, C. J. Pérez Vicente, F. Ritort, and R. Spigler. *Rev. Mod. Phys.*, 77:137–185, 2005.
- [33] C. W. Wu. *Synchronization in Complex Networks of Nonlinear Dynamical Systems*. World Scientific, 2007.
- [34] J. D. Crawford and K. T. R. Davies. *Physica D*, 125:1–46, 1999.
- [35] R. E. Mirollo and S. H. Strogatz. *J. Stat. Phys.*, 60(1/2):245–261, 1990.
- [36] B. Sonnenschein, L. Schimansky-Geier, and F. Sagués. *In preparation*.
- [37] B. R. Preiss. *Data Structures and Algorithms with Object-Oriented Design Patterns in C++*. Wiley & Sons, 1998.
- [38] D. J. Watts and S. H. Strogatz. *Nature*, 393:440–442, 1998.
- [39] M. E. J. Newman and D. J. Watts. *Phys. Rev. E*, 60(6):7332–7342, 1999.
- [40] R. Mannella. A Gentle Introduction to the Integration of Stochastic Differential Equations. In J. A. Freund and T. Pöschel, editors, *Stochastic Processes in Physics, Chemistry, and Biology*, volume 557, pages 353–364. Springer-Verlag, Berlin Heidelberg, 2000.